

Supplementary Materials

Microwave-assisted synthesis of defective $\text{Ca}_{1-x}\text{Ag}_x\text{Ti}_{1-y}\text{Co}_y\text{O}_3$ with high photoelectrocatalysis activity for organic pollutants removal from water

Chen Chen ^a, Jiamei Zhao ^a, Dong Guo ^b, Keyu Duan ^a, Yongqiang

Wang ^a, Xiaowen Lun ^{*a}, Conglu Zhang ^{**a}

^a School of Pharmaceutical Engineering, Shenyang Pharmaceutical University,
Benxi, Liaoning Province 117004, PR China

^b Beijing Normal University, Beijing 100875, PR China

Caption

- 1. Text S1. The details of the microwave instrument. (Page 3)**
- 2. Text S2. Detailed structural information of XRD. (Page 4)**
- 2. Fig. S1. Photoelectrocatalysis reaction device. (Page 5)**
- 3. Fig. S2. Self-designed quartz reactor. (Page 6)**
- 4. Fig. S3. Color comparison of CaTiO_3 with different Ag doping amounts:(a) 0 wt%; (b) 2 wt%; (c) 4 wt%; (d) 4 wt%. (Page 7)**
- 5. Fig. S4. XRD patterns for $\text{Ca}_{1-x}\text{Ag}_x\text{Ti}_{1-y}\text{Co}_y\text{O}_3$ before and after photoelectric catalytic reactions. (Page 8)**
- 6. Table S1. Comparison of Interplanar Spacing (d) between CaTiO_3 and $\text{Ca}_{1-x}\text{Ag}_x\text{Ti}_{1-y}\text{Co}_y\text{O}_3$. (Page 9)**
- 7. Table S2. Comparison of Lattice Parameters and Cell Volume of CaTiO_3 and $\text{Ca}_{1-x}\text{Ag}_x\text{Ti}_{1-y}\text{Co}_y\text{O}_3$. (Page 10)**
- 8. Table S3. Various Structural Parameters of CaTiO_3 and $\text{Ca}_{1-x}\text{Ag}_x\text{Ti}_{1-y}\text{Co}_y\text{O}_3$. (Page 11)**
- 9. Table S4. XPS peak splitting parameters of Ag 3d. (Page 12)**
- 10. Table S5. Relative distribution of the oxidation states of Co on the surface of $\text{Ca}_{1-x}\text{Ag}_x\text{Ti}_{1-y}\text{Co}_y\text{O}_3$ catalysts. (Page 13)**

Text S1. The details of the microwave instrument.

The microwave instrument (TANK eco, SINEO, Shanghai) frequency was 2450 MHz. Sample reaction containers were made of chemical resistant material (strengthened poly tetra fluoroethylene, TFM). The microwave instrument adopts multi-core integrated optical fiber and infrared dual temperature measurement system, temperature range: -40~305°C, accuracy $\pm 0.1^\circ\text{C}$.

Text S2. Detailed structural information of XRD.

Table S1 shows the interplanar distances (d) of crystals, which are estimated according to Bragg's equation (Eq. 1).

$$n\lambda = 2dsin \theta \quad (1)$$

where θ is symbolized for Bragg's angle of a particular diffraction peak and λ represents the wavelength of Cu $K\alpha$ radiation. The lattice parameters (a, c) along with unit cell volume (V) of the CaTiO_3 and $\text{Ca}_{1-x}\text{Ag}_x\text{Ti}_{1-y}\text{Co}_y\text{O}_3$ are calculated via lattice geometry Eqs. 2 and 3, respectively.

$$\frac{l}{d^2} = \frac{h^2}{a^2} + \frac{k^2}{b^2} + \frac{l^2}{c^2} \quad (\text{Orthorhombic phase}) \quad (2)$$

$$V = abc \quad (3)$$

The values of desired structural lattice parameters and unit cell volume for all samples are given in Table S2. From Scherrer's equation (Eq. 4) and Eq. 5, the average crystallite size (D) and microstrain (ε), of all materials are evaluated through experimental XRD data. The microstrain signify that some defects are present in the material.

$$D = \frac{k\lambda}{\beta \cos \theta} \quad (4)$$

$$\varepsilon = \frac{\beta \cos \theta}{4} \quad (5)$$

β is a full width at half maxima of the respective peak in radian and k symbolized for shape factor, equal to 0.89. The structural parameters of all samples are given in Table S3.

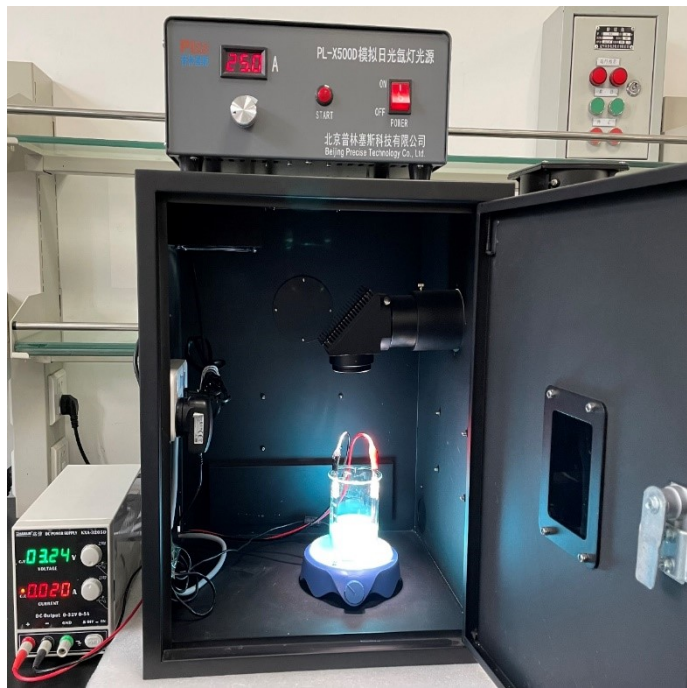


Fig. S1. Photoelectrocatalysis reaction device.



Fig. S2. Self-designed quartz reactor.

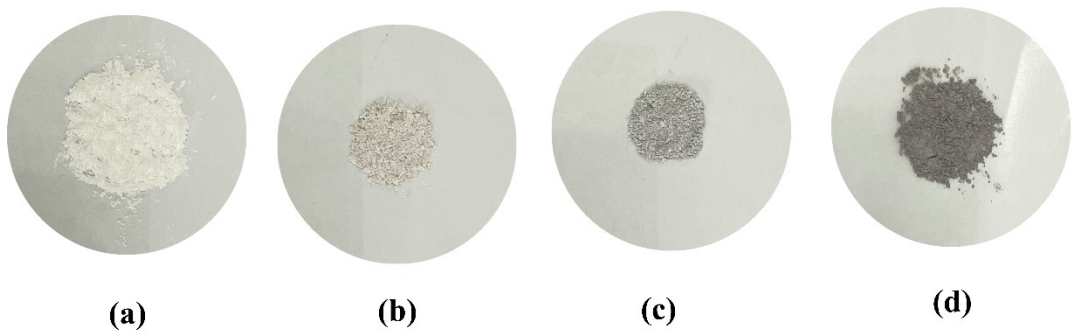


Fig. S3. Color comparison of CaTiO₃ with different Ag doping amounts:

(a) 0 wt%; (b) 2 wt%; (c) 4 wt%; (d) 4 wt%.

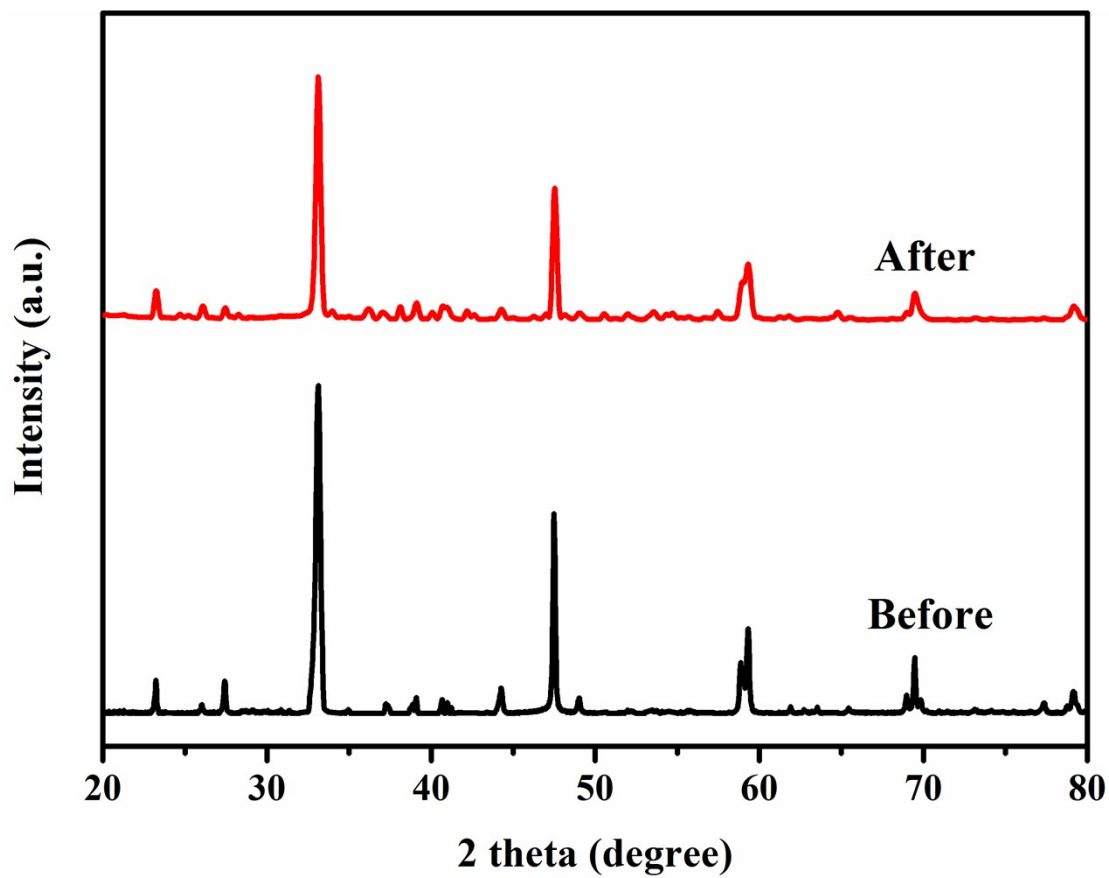


Fig. S4. XRD patterns for $\text{Ca}_{1-x}\text{Ag}_x\text{Ti}_{1-y}\text{Co}_y\text{O}_3$ before and after photoelectric catalytic reactions.

Table S1. Comparison of Interplanar Spacing (d) between CaTiO₃ and Ca_{1-x}Ag_xTi_{1-y}Co_yO₃.

(hkl) planes	Standard (Å)	interplanar distance (d)	
		CaTiO ₃	observed (Å) Ca _{1-x} Ag _x Ti _{1-y} Co _y O ₃
(101)	3.8283	3.8979	3.9075
(111)	3.4231	3.5041	3.5116
(121)	2.7050	2.8166	2.8202
(130)	2.3010	2.4400	2.4468
(202)	1.9142	2.0876	2.0897
(212)	1.8569	2.0399	2.0411
(321)	1.5565	1.7931	1.7942
(242)	1.3525	1.6445	1.6451
(161)	1.2090	1.5683	1.5686

Table S2. Comparison of Lattice Parameters and Cell Volume of CaTiO₃ and Ca_{1-x}Ag_xTi_{1-y}Co_yO₃.

		observed	
lattice parameters	standard	CaTiO ₃	Ca _{1-x} Ag _x Ti _{1-y} Co _y O ₃
a (Å)	5.3829	6.0423	6.1279
b (Å)	7.6453	8.0012	8.0064
c (Å)	5.4458	5.1084	5.0728
volume (Å ³)	224.1158	246.9689	248.8838

Table S3. Various Structural Parameters of CaTiO₃ and Ca_{1-x}Ag_xTi_{1-y}Co_yO₃.

structural parameters	CaTiO ₃	Ca _{1-x} Ag _x Ti _{1-y} Co _y O ₃
crystallite size (D) (nm)	31.4919	39.7075
microstrain (ϵ) ($\times 10^{-3}$)	1.1933	1.0549

Table S4. XPS peak splitting parameters of Ag 3d.

	X ₀ (center)	A (area)	W (fwhm)
Peak 1 (Ag ⁰)	368.0	10455.28	3.336
Peak 2 (Ag ⁺)	368.1	32553.83	1.152
Peak 3 (Ag ⁰)	373.7	9565.60	3.086
Peak 4 (Ag ⁺)	374.0	20654.51	1.089

Table S5. Relative distribution of the oxidation states of Co on the surface of

Ca_{1-x}Ag_xTi_{1-y}Co_yO₃ catalysts.

Sample	Oxidation state of Co (percentage)		
	Co ²⁺	Co ³⁺	Co ⁴⁺
Ca _{1-x} Ag _x Ti _{1-y} Co _y O ₃	44.22	24.67	31.11